Charge transfer interaction in the acetic acid–benzene cation complex

Kentaroh Kosugi, Yoshiya Inokuchi, and Nobuyuki Nishi[a)]
Institute for Molecular Science, and School of Mathematical and Physical Science, The Graduate University for Advanced Studies, Okazaki National Research Institutes, Myodaiji, Okazaki 444-8585, Japan

(Received 4 October 2000; accepted 19 December 2000)

Geometrical and electronic structures of the acetic acid–benzene cation complex, $(CH_3COOH)\cdot(C_6H_6)^+$, are studied experimentally and theoretically. Experimentally, a vibrational spectrum of $(CH_3COOH)\cdot(C_6H_6)^+$ in the supersonic jet is measured in the 3000–3680 cm^{-1} region using an ion-trap photodissociation spectrometer. An electronic spectrum is also observed with this spectrometer in the 12 000–29 600 cm^{-1} region. Theoretically, *ab initio* molecular orbital calculations are performed for geometry optimization and evaluation of vibrational frequencies and electronic transition energies. The vibrational spectrum shows two distinct bands in the O–H stretching vibrational region. The frequency of the strong band (3577 cm^{-1}) is close to that of the O–H stretching vibration of acetic acid and the weak one is located at 3617 cm^{-1}. On the basis of geometry optimizations and frequency calculations, the strong band is assigned to the O–H stretching vibration of the *cis*-isomer of acetic acid in the hydrogen-bonded complex (horizontal *cis*-isomer). The weak one is assigned to the vertical *trans*-isomer where the *trans*-isomer of acetic acid interacts with the π-electron system of the benzene cation. The weakness of the high frequency band in the photodissociation spectrum is attributed to the binding energy larger than the photon energy injected. Only hot vertical *trans*-isomers can be dissociated by the IR excitation. The electronic spectrum exhibits two bands with intensity maxima at 17 500 cm^{-1} and 24 500 cm^{-1}. The calculations of electronic excitation energies and oscillator strengths suggest that charge transfer bands of the vertical *trans*-isomer can be observed in this region in addition to a local excitation band of the horizontal *cis*-isomer. We assign the 17 500 cm^{-1} band to the charge transfer transition of the vertical *trans*-isomer and the 24 500 cm^{-1} band to the $\pi-\pi$ transition of the horizontal *cis*-isomer. The calculations also suggest that the charge transfer is induced through the intermolecular C···O═C bond formed between a carbon atom of benzene and the carbonyl oxygen atom of acetic acid. © *2001 American Institute of Physics.* [DOI: 10.1063/1.1349082]

I. INTRODUCTION

Intermolecular interaction is a principal subject of chemistry for understanding the nature of substances and chemical reactions. For example, the O–H···O and N–H···O hydrogen-bonding interactions are very important as well as hydrophobic interaction in structural biology. In recent years, other types of intermolecular interactions have been recognized to play important roles in biological macromolecules. Derewenda and co-workers reported that not only classical hydrogen bonds that involve electronegative nitrogen and oxygen atoms but also the C–H···O hydrogen bond must be considered in the determination of protein structures.[1] The C–H···O hydrogen bond is also important for cluster structures in aqueous solutions.[2–4] Gallivan and Dougherty showed that cation-π interactions are frequently found on the surfaces of proteins, exposed to aqueous solvation and can effect the protein structures.[5] Caldwell and Kollman indicated that charge transfer is important in an accurate description of the cation-π interaction.[6] These studies suggest that quantitative understanding of the charge transfer interactions between fundamental molecules of biological importance is indispensable particularly for the study of protein structures and functions.

Generation of charge transfer complexes in supersonic jet is favorable for the studies of the charge transfer interaction in a molecule pair, since these are cooled and isolated from solvation. In the electronic spectra of the charge transfer complexes, new bands appear due to the intermolecular charge transfer interaction. These bands are called charge transfer (CT) bands. An electronic ground state of a charge transfer ion complex composed of molecules A and B is described by the wave function, $\Psi_G = a\psi(A)\psi(B^+) + b\psi(A^+)\psi(B)$. In the case where the ionization potential of A is higher than that of B, $|a| > |b|$. The electronic transition from the ground state to an excited state [described by the wave function, $\Psi_E = c\psi(A)\psi(B^+) + d\psi(A^+)\psi(B)$] accompanies the change in intermolecular charge distribution. CT bands arise from this kind of the transitions. The transition probability of the CT band depends on the degree of intermolecular charge transfer and, thereby, the geometrical structure of the complex. CT bands of the cation complexes with two aromatic molecules have been measured by photodissociation spectroscopy.[7–9] The CT band of the benzene–naphthalene heterodimer cation is observed at 10 870 cm^{-1}.[7] In the spectrum of the benzene–toluene heterodimer ion,

a)Author to whom correspondence should be addressed. Electronic mail: nishi@ims.ac.jp

three CT bands are seen at 8510, 10 870, and 14 925 cm^{-1}.[8] Ohashi *et al.* measured vibrational and electronic spectra of the benzene–benzyl alcohol heterodimer ion by photodissociation spectroscopy and observed the CT band at 10 525 cm^{-1}.[9] From the observation of the hydroxyl group stretching vibration free from intermolecular perturbations at 3662 cm^{-1}, the geometrical structure of the cation complex is attributed to a sandwichlike structure suitable for the charge transfer interaction. Geometrical structures of these cation complexes that show the CT bands are characterized with overlapping of the π-electron systems of the respective aromatic rings. This situation is similar to the benzene dimer cation that shows intermolecular charge resonance (CR) bands in the near-infrared region.[10–12] In contrast, the CT band is not observed in the spectra of the cation complexes with dominant hydrogen-bonding interactions. The electronic spectrum of the benzene–phenol heterodimer cation shows the lack of the CT band.[13] Fujii *et al.* observed the vibrational spectrum of the benzene–phenol heterodimer ion.[14] They found an extremely large redshift and a substantial broadening of the O–H stretching vibrational band. The result indicates that the cation complex has a structure with a hydrogen bond between the O–H bond of phenol and the π-electrons of benzene. Ohashi *et al.* reported that no CT band can be seen in the electronic spectrum of the aniline–benzene heterodimer ion.[15] Aniline–benzene heterodimer ions are also reported to have hydrogen-bonded structures, where aniline is bound to benzene through a π-type hydrogen bond.[16] In these dimer ions, the hydrogen-bonding interaction overwhelms the charge transfer interaction.

In the present paper, we report the intermolecular interactions between the carboxyl group and the cationic benzene ring in the acetic acid–benzene heterodimer cation. The ionization potentials of acetic acid and benzene are 10.87 (Ref. 17) and 9.24 eV,[18] respectively. The positive charge is expected to be localized at the benzene ring in the ground state, because of the large difference in the ionization potentials.[8] Thus we abbreviate the acetic acid–benzene heterodimer cation as $(CH_3COOH)\cdot(C_6H_6)^+$ hereafter. Since the carboxyl group exists in a large number of biologically important molecules, understanding of its interaction with ionic molecules is very important. Molecules with carboxyl groups are expected to show specific hydrogen-bonding interaction with other hydrogen-donating or accepting molecules.[2–4,19,20] Nonbonding orbitals of the carboxyl group may interact with the positively charged π-electron system. We investigate the geometrical structures and electronic states of $(CH_3COOH)\cdot(C_6H_6)^+$, experimentally and theoretically. In order to obtain information on the geometrical structures, the vibrational spectrum of $(CH_3COOH)\cdot(C_6H_6)^+$ was measured in the 3000–3680 cm^{-1} region by using the photodissociation spectroscopy. We also performed *ab initio* molecular orbital calculations. The calculated frequencies of the optimized geometries are compared with the experimental spectrum to clarify the structures of $(CH_3COOH)\cdot(C_6H_6)^+$. On the basis of the optimized geometrical structures, we carried out the calculations of the electronic transition energies to find the nature of the two broad electronic bands observed in the 12 020–13 405 cm^{-1} and 14 925–29 410 cm^{-1} regions.

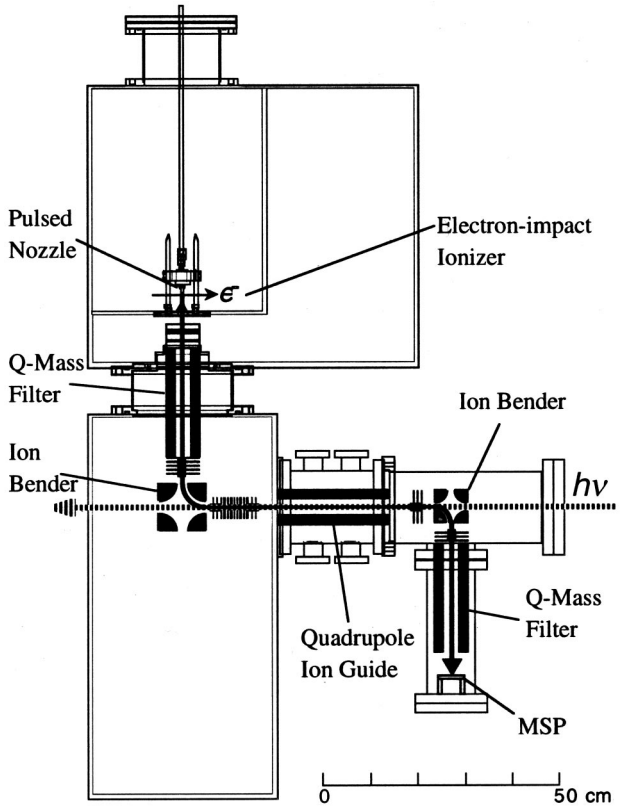

FIG. 1. Schematic diagram of the vacuum system and the tandem mass spectrometer for photodissociation spectroscopy.

II. EXPERIMENT

Figure 1 shows a schematic diagram of the ion trap system used for the IR photodissociation spectroscopy of cluster ions. The mixture of acetic acid and benzene was prepared by flowing the carrier Ar gas over liquid benzene and liquid acetic acid situated separately in the respective sample folders. The former was located 2 m away and the latter was 5 cm to a pulsed nozzle (General Valve P/N 9-279-900). The mixture of the sample and the carrier gas was then introduced and expanded into the vacuum chamber through the pulsed nozzle. The total stagnation pressure was 1.1×10^5 Pa. Neutral clusters were ionized by electron-impact with an electron energy of 350 eV near the exit hole of the pulsed nozzle. The ions, $(CH_3COOH)\cdot(C_6H_6)^+$, of interest were selected by a quadrupole mass filter. Then the ion beam was deflected 90° by a quadrupole ion bender and introduced into a quadrupole ion guide. IR or visible laser beam propagated coaxially along the quadrupole and irradiated the trapped ions. The excited cluster ions with sufficient energy for the dissociation can produce benzene monomer cations as a fragment species. The fragment cations were deflected 90° by another quadrupole ion bender and mass-analyzed with the third quadrupole mass filter connected to a secondary electron multiplier. Photodissociation spectra were obtained by recording the yields of the fragments against the excitation energies. The tunable light source for the IR region was a optical parametric oscillator (OPO) system (Continuum Mirage 3000) pumped with an injection-seeded Nd:YAG la-

ser (Continuum Powerlite 9000). The resolution of the OPO laser was less than 0.02 cm^{-1}. This laser system was also used in the 12 020–13 405 cm^{-1} (746–832 nm) region. A dye laser (Lambda Physik LPD3000) pumped with an excimer laser (Lambda Physik LPX100) was used in the 14 925–29 410 cm^{-1} (340–670 nm) region. Spectroscopy grade acetic acid and benzene were purchased from Wako Pure Chemical Company and used without further purification.

III. COMPUTATIONAL DETAILS

Ab initio molecular orbital calculations were performed using the GAUSSIAN 98W program package[21] and the PC GAMESS version[22] of the GAMESS (US) QC package[23] on commercial computers. The Pople's 6-31G(d,p) basis set was employed for all the calculations. The ground state optimized geometries and their vibrational frequencies were determined by the CASSCF calculations. Seven π electrons were treated as active electrons and distributed among seven active orbitals. The active orbitals of benzene cation consist of two bonding π and two antibonding π^* orbitals, and those of acetic acid are a bonding π, an antibonding π^* and one of nonbonding orbitals. Geometry optimizations and vibrational frequency evaluation were also carried out by the calculations based on the density functional theory (DFT) in which Becke's three-parameter hybrid functional[24] are combined with the Lee–Yang–Parr (LYP) correlation functional[25,26] (B3LYP).

The ground and excited state energies of the complexes with the geometries optimized at the CASSCF(7,7) level were calculated by the state-averaged CASSCF method and the second-order multiconfiguration quasidegenerate perturbation theory (MCQDPT).[27] For these calculations, we extended the active space by adding four electrons and three orbitals (bonding σ, π, and antibonding π^* orbitals) to the active space mentioned above: the state-averaged CASSCF(11, 10) and MCQDPT(11, 10) calculations. In order to know the electron distribution between component molecules in the ground and excited states of isomer complexes, Mulliken population analysis[28–31] was carried out for the respective electronic states. Radiative transition dipole moments and oscillator strengths between the ground and excited states were also calculated at the state-averaged CASSCF(11, 10) level. Molecular orbitals shown in this paper were pictured by using MacMolPlt.[32]

IV. RESULTS AND DISCUSSION

A. Geometrical structures of $(CH_3COOH)\cdot(C_6H_6)^+$ isomers

1. Vibrational spectra

Figure 2 exhibits an IR photodissociation spectrum of $(CH_3COOH)\cdot(C_6H_6)^+$ in the region of 3000–3680 cm^{-1}. With our OPO system, laser intensity in the region lower than 3000 cm^{-1} was not strong enough to produce any reliable photodissociation spectrum of the complex. Three bands are observed in this region. In the O–H stretching vibrational region, a weak band is also seen on the high frequency side of the strongest band. They are located closely and overlap with each other. The doublet spectrum is decomposed into two bands by fitting two Lorentzians (dotted curves) to the observed data as shown in Fig. 3. The decomposition reveals that the positions of the intensive band and the weak one are located at 3577 and 3617 cm^{-1}, respectively. Another weak band is also observed in the C–H stretching vibrational region. The frequency of the band is 3080 cm^{-1}.

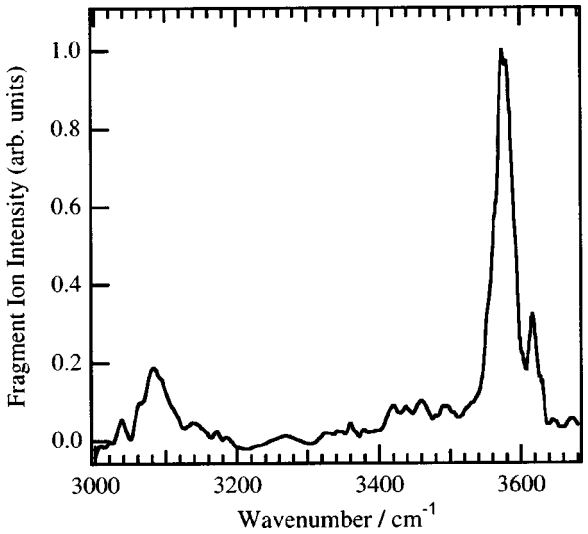

FIG. 2. Vibrational spectrum of $(CH_3COOH)\cdot(C_6H_6)^+$ in the region of 3000–3680 cm^{-1} obtained by photodissociation spectroscopy.

The complex of $(CH_3COOH)\cdot(C_6H_6)^+$ has two types of C–H bonds; one is that of benzene monomer cation and the other is that of acetic acid. In most cases, the frequencies of the C–H stretching vibrations of an aromatic ring are higher than that of a methyl group. It is difficult to observe acetic acid monomers in supersonic jet because of the high stability of the cyclic dimers in gas phase. Thus, IR spectra of acetic acid monomer species were observed at 150 and 175 °C. Weltner observed three C–H stretching vibrational bands at 2935, 2983, and 3027 cm^{-1}.[33] Haurie and Novak also ob-

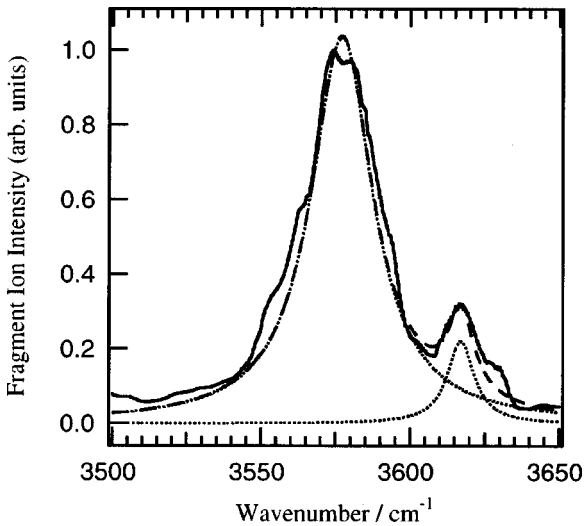

FIG. 3. Decomposition of the vibrational spectrum in the O–H stretching region. The doublet spectrum is decomposed into two bands by fitting two Lorentzians (dotted curves) whose centers are at 3577 and 3617 cm^{-1}. The sum of these Lorentzians is also shown with a broken line.

served the IR spectrum of gaseous acetic acid where the C–H stretching bands are located 2944, 2996, and 3051 cm^{-1} (Ref. 34) in accord with the previously reported frequencies of 2961, 2997, and 3048 cm^{-1},[35] respectively. On the other hand, the C–H stretching vibrations of benzene were observed using supersonic jet technique. Using IR–UV double resonance spectroscopy, Lee and co-workers observed three bands at 3048, 3079, and 3101 cm^{-1} in the C–H stretching region of neutral benzene.[36] They explained the three bands in terms of the Fermi resonance among one IR-active C–H stretching vibration and two combination bands of the in-plane vibrations. Fujii *et al.* observed an IR spectrum of benzene monomer cation using the messenger technique.[37] They observed only a single band at 3094 cm^{-1} in the C–H stretching region. According to these investigations, one can expect the C–H stretching vibrations of acetic acid in the region from 2935 to 3051 cm^{-1} and that of benzene at 3094 cm^{-1}. In the IR spectrum of $(CH_3COOH)\cdot(C_6H_6)^+$, the frequencies of some C–H stretching vibrations coupled with intermolecular binding can be redshifted due to the cluster formation. The band at 3080 cm^{-1} observed in our spectrum is assigned to a C–H stretching vibration of the benzene molecule in $(CH_3COOH)\cdot(C_6H_6)^+$.

The O–H stretching vibration of a carboxyl group is only responsible for the strong band observed in the region over 3500 cm^{-1}. The appearance of the two bands at 3577 and 3617 cm^{-1} suggests the two possibilities of either the presence of two isomers or Fermi resonance intensity enhancement of a combination band. Here we disregard the latter possibility because acetic acid has little possibility showing any combination band at 3617 cm^{-1}. There is no combination of vibrational frequencies responsible for the Fermi resonance. In fact, no Fermi resonance band is reported in this region.[34,35] Thus the doublet can be originated from two distinct geometries of $(CH_3COOH)\cdot(C_6H_6)^+$. The O–H stretching vibration of an acetic acid monomer was observed at 3577 cm^{-1} in gas phase by Wilmshurst.[35] Haurie and Novak observed the same band at 3583 cm^{-1}.[34] The discrepancy in the frequencies is probably due to the broadness of the band with enhanced rotational envelopes at high temperatures. The frequency of the strong band (3577 cm^{-1}) is just the same as that of the acetic acid monomer and assigned to the free O–H stretching vibration of $(CH_3COOH)\cdot(C_6H_6)^+$. The frequency of the weak band (3617 cm^{-1}) is 40 cm^{-1} higher than that of the strong band. This suggests that the O–H bond of the isomer is stronger than that of the 3577 cm^{-1} band and can be completely free from hydrogen-bonding. The O–H bond of the carboxyl group is affected by weak intramolecular hydrogen-bonding interaction with the carbonyl oxygen. The isomer with a geometry where the intramolecular hydrogen bond is weaker than that of the observed acetic acid monomer species can be responsible for the weak band at 3617 cm^{-1}.

There are two isomers for the acetic acid monomer as shown in Fig. 4: the hydroxyl hydrogen and the carbonyl oxygen located on the same side of the C–O single bond (*cis*-isomer) and on the opposite side (*trans*-isomer). The hydroxyl group of the *cis*-isomer is stabilized due to intramolecular hydrogen-bonding interaction with the carbonyl oxygen. In contrast to this, the hydroxyl group of *trans*-isomer is almost free, therefore the O–H stretching frequency of the *trans*-isomer is expected to be higher than that of the *cis*-isomer. Turi and Dannenberg studied these isomers by *ab initio* molecular orbital calculations.[38] They reported the frequency of the O–H stretching vibration of the *trans*-isomer is 59.6 cm^{-1} higher than that of the *cis*-isomer at the MP2/6-31G(d) level. Thus the weak band at 3617 cm^{-1} can be assigned to the O–H stretching vibration of the *trans*-isomer in the cation complex. However, only the *cis*-isomer is observed in the vibrational spectrum of the acetic acid monomer because the ground state energy of the *trans*-isomer is higher than that of the *cis*-isomer. The energy difference was calculated to be 6.1 kcal/mol at the MP2/6-31G(d,p) level.[38] In a complex of $(CH_3COOH)\cdot(C_6H_6)^+$, one can expect the intermolecular interaction of the *trans*-isomers with the benzene monomer cation at the oxygen atoms of the carbonyl and the hydroxyl groups, since the *trans*-isomer has the space faced by the two oxygen atoms for the complex formation. In this case, the total energy of the complex with the *trans*-isomer can be lowered much more than that of the *cis*-isomer. Our assignment should be reinforced with the *ab initio* molecular orbital calculations with sufficient reliability.

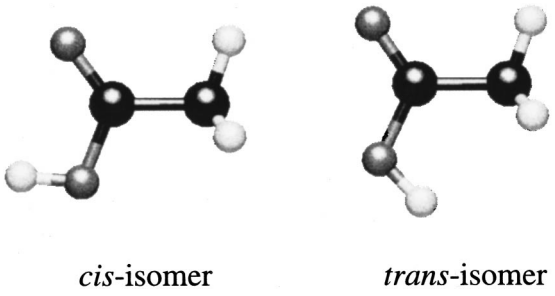

FIG. 4. Two isomers of acetic acid. The *cis*-isomer (left) is stabilized by intramolecular hydrogen-bonding interaction between the carbonyl oxygen and the hydroxyl hydrogen; consequently, it is more stable than the *trans*-isomer (right). A black ball stands for a carbon atom, gray one is oxygen, and white one represents a hydrogen atom.

2. Calculated structures and binding energies

Geometry optimizations were carried out with various initial structures of C_s symmetry or C_1 symmetry which include one of the two isomers of acetic acid. In consequence, three stationary points were found at the CASSCF(7,7) level. All the optimized structures at these minima have a C_s plane on which the acetic acid molecule is sitting except for two methyl hydrogens located symmetrically above and under the plane. These structures displayed in Fig. 5 are classified into the two types distinguished by the relative position of the carboxyl group to the benzene ring. One is a horizontal complex in which an acetic acid molecule and a benzene cation are situated on the same plane forming hydrogen bonds between the carboxyl oxygen and the two hydrogen atoms of the benzene ring. The other is a vertical complex where the carboxyl plane is at a right angle with the benzene plane and the carboxyl oxygen directly interacts with the π-electron system of the benzene cation. For each type of the

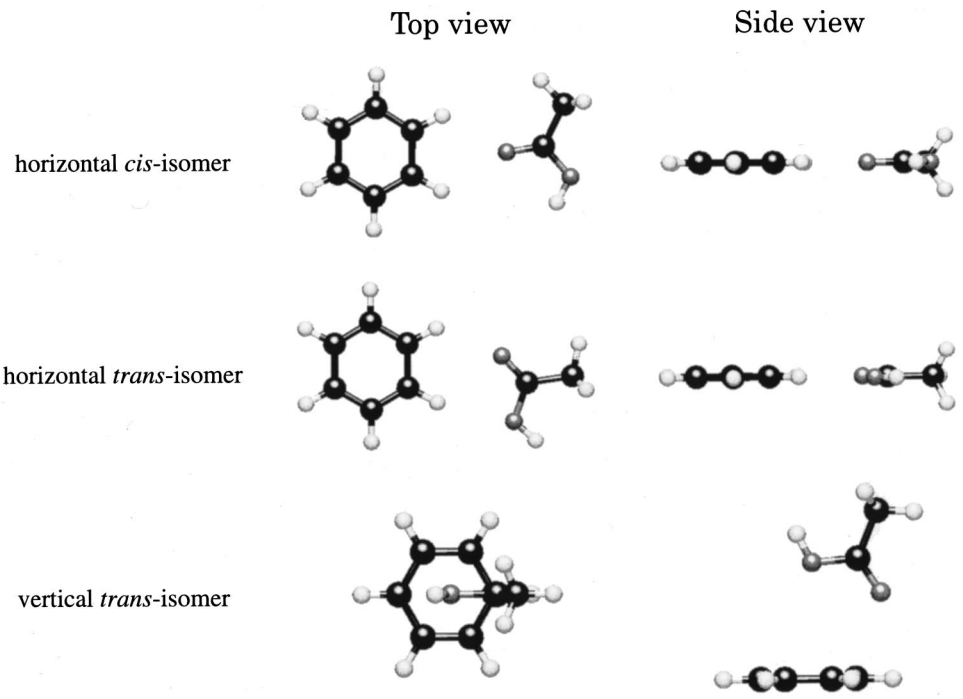

FIG. 5. Geometrical structures of $(CH_3COOH)\cdot(C_6H_6)^+$ optimized at the CASSCF(7,7)/6-31G(d,p) level. The three structures (the horizontal *cis*-isomer, the horizontal *trans*-isomer, and the vertical *trans*-isomer) are found to be at minima on the potential surface in agreement with those obtained at the B3LYP/6-31G(d,p) level. Each of these structures is viewed from the top and the side of the benzene ring.

complexes, two isomers containing a *cis*-isomer or a *trans*-isomer of acetic acid are expected. In the case of the horizontal complex, both of the isomers are found to have their own optimized geometries. ''Horizontal *cis*-isomer'' designates the one containing the *cis*-isomer and the other with the *trans*-isomer is called ''horizontal *trans*-isomer.'' On the other hand, the *trans*-isomer is the only structure at a minimum of the vertical complex: the vertical *trans*-isomer. The vertical *cis*-isomer structure exhibits a saddle point with imaginary frequencies.

The calculated total energies of the optimized structures of $(CH_3COOH)\cdot(C_6H_6)^+$ and the energies relative to the most stable species at the CASSCF(7,7)/6-31G(d,p) level are shown in Table I. We corrected those for zero-point vibrational energies (ZPVE) and they are displayed in Table I. The most stable complex species is the vertical *trans*-isomer. The horizontal *cis*-isomer is the second stable species and 2459 and 2621 cm^{-1} less stable than the vertical *trans*-isomer before and after ZPVE correction, respectively. The least stable species is the horizontal *trans*-isomer that is 2936 and 3053 cm^{-1} less stable than the vertical *trans*-isomer before and after ZPVE correction, respectively.

We also carried out the geometry optimization on the two isomers of acetic acid and a benzene cation. The total energies of these monomer species before and after ZPVE correction are listed in Table II. As already mentioned, the *trans*-isomer of acetic acid is less stable than the *cis*-isomer. The repulsive interaction between the hydroxyl hydrogen and the methyl group of *trans*-isomer also contributes to the instability of the *trans*-isomer. As shown in Table III, the energy gap between the *cis*- and *trans*-isomers of acetic acid is 2210 cm^{-1} (6.32 kcal/mol) and 2116 cm^{-1} (6.05 kcal/mol) at the CASSCF(7,7)/6-31G(d,p) level before and after ZPVE correction, respectively. Our result is in good agreement with the value of 6.1 kcal/mol calculated by Turi and Dannenberg at the MP2/6-311++G(d,p) level without ZPVE correction.[38] The large energy gap prevents the *trans*-isomer from being observed in gas and liquid phase.

For $(CH_3COOH)\cdot(C_6H_6)^+$, the energy gap between the horizontal *cis*-isomer and the horizontal *trans*-isomer is also

TABLE I. Total energies (hartree) and energy gaps relative to the most stable species (cm^{-1}) of $(CH_3COOH)\cdot(C_6H_6)^+$ at the CASSCF(7,7)/6-31G(d,p) and B3LYP/6-31G(d,p) levels.

		Horizontal *cis*	Horizontal *trans*	Vertical *trans*
CASSCF(7,7)/6-31G(d,p)				
without ZPVE correction	total energy	−458.319 530	−458.317 354	−458.330 733
	energy gap	2459	2936	0
after ZPVE correction	total energy	−458.147 229	−458.145 260	−458.159 172
	energy gap	2621	3053	0
B3LYP/6-31G(d,p)				
without ZPVE correction	total energy	−461.044 106	−461.040 888	−461.048 177
	energy gap	894	1600	0
after ZPVE correction	total energy	−460.883 041	−460.879 404	−460.885 483
	energy gap	536	1334	0

TABLE II. Total energies (hartree) of the benzene monomer cation and acetic acid monomers at the CASSCF(7,7)/6-31G(d,p) and B3LYP/6-31G(d,p) levels.

	Benzene monomer cation	Acetic acid	
		cis	*trans*
CASSCF(7,7)/6-31G(d,p)			
without ZPVE correction	−230.442 057	−227.848 701	−227.838 632
after ZPVE correction	−230.337 077	−227.782 392	−227.772 750
B3LYP/6-31G(d,p)			
without ZPVE correction	−231.932 185	−229.091 479	−229.081 701
after ZPVE correction	−231.834 320	−229.029 469	−229.020 016

shown in Table III. The values are 477 cm^{-1} (1.36 kcal/mol) and 432 cm^{-1} (1.24 kcal/mol) at the CASSCF(7,7)/6-31G(d,p) level before and after ZPVE correction, respectively. The energy gap of the horizontal cluster is only 20% of that of acetic acid at the CASSCF(7,7)/6-31G(d,p) level after ZPVE correction. As we shall see later, the geometrical differences of the acetic acid isomers from those in the horizontal clusters are not large enough to explain the drastic change in the energy gap. Therefore, the large change in the stabilization energies is attributed to the intermolecular binding energies of the horizontal clusters.

Table IV shows the binding energies of the geometry optimized complexes of $(CH_3COOH)\cdot(C_6H_6)^+$ at the CASSCF(7,7)/6-31G(d,p) level. The binding energy is defined as the difference of the total energy of $(CH_3COOH)\cdot(C_6H_6)^+$ from the sum of the component monomer energies. Corrected energies for ZPVE are also shown in Table IV. The binding energy of the horizontal *cis*-isomer is 6315 cm^{-1} (18.06 kcal/mol, 0.78 eV) and 6093 cm^{-1} (17.42 kcal/mol, 0.75 eV) before and after ZPVE correction, respectively. On the other hand that of the horizontal *trans*-isomer is 8047 cm^{-1} (23.01 kcal/mol, 1.00 eV) and 7777 cm^{-1} (22.24 kcal/mol, 0.96 eV) before and after ZPVE correction, respectively. This indicates that the conformational change of the carboxyl group produces large difference in the strength of the intermolecular interaction and the *trans*-isomer is much preferable for the in-plane intermolecular interaction between acetic acid and benzene monomer cation. The binding energy of the vertical *trans*-isomer is 10 984 cm^{-1} (31.40 kcal/mol, 1.36 eV) and 10 830 cm^{-1} (30.96 kcal/mol, 1.34 eV) before and after ZPVE correction, respectively. The intermolecular bond in the vertical *trans*-isomer is about 1.4 times stronger than that of the horizontal *trans*-isomer. This means that the intermolecular interaction in the vertical complex has a nature different from the hydrogen-bonding interaction seen in the horizontal complexes.

TABLE III. Energy gaps (cm^{-1}) between the *cis*- and *trans*-isomers at the CASSCF(7,7)/6-31G(d,p) and B3LYP/6-31G(d,p) levels.

	Horizontal cluster	Acetic acid monomer
CASSCF(7,7)/6-31G(d,p)		
without ZPVE correlation	477	2210
after ZPVE correlation	432	2116
B3LYP/6-31G(d,p)		
without ZPVE correlation	706	2146
after ZPVE correlation	798	2075

TABLE IV. Binding energies (cm^{-1}) of $(CH_3COOH)\cdot(C_6H_8)^+$ at the CASSCF(7,7)/6-31G(d,p) and B3LYP/6-31G(d,p) levels.

	Horizontal		Vertical
	cis	*trans*	*trans*
CASSCF(7,7)/6-31G(d,p)			
without ZPVE correlation	6315	8047	10 984
after ZPVE correlation	6093	7777	10 830
B3LYP/6-31G(d,p)			
without ZPVE correlation	4487	5926	7526
after ZPVE correlation	4225	5502	6836

The point is that the *trans*-isomer of acetic acid is preferable to the *cis*-isomer not only for the formation of the vertical complex but also for the horizontal complexes. Geometrical change of the component molecules upon the complex formation reflects the change of electron density. Geometrical parameters of intermolecular lengths give information on the character of the intermolecular bonding. Therefore, let us consider this point from the optimized geometrical parameters of the complex cations and acetic acid monomers. The optimized geometrical parameters of three isomers of $(CH_3COOH)\cdot(C_6H_6)^+$ and two isomers of acetic acid at the CASSCF(7,7)/6-31G(d,p) level are collected in Table V. To start with, we compare those of the horizontal *cis*-isomer with those of the horizontal *trans*-isomer. The C–H bond lengths of the methyl groups of both the horizontal complexes are almost equal to those of the acetic acid monomers. This result indicates that the intermolecular interaction does not affect the electron density of the methyl group. The intermolecular bond lengths between the carbonyl oxygen and the first and the second nearest hydrogen atoms of the benzene cation are 2.3862 and 2.4508 Å, respectively, for the horizontal *cis*-isomer. Those for the horizontal *trans*-isomer are 2.3218 and 2.5962 Å, respectively. These indicate that the carbonyl oxygens of both the horizontal complexes form double hydrogen bonds with two of the hydrogens of the benzene cations. Because of the hydrogen bonds at the carbonyl group, the C═O bonds of the horizontal complexes are longer than those of the acetic acid monomers.

There are important differences between the horizontal *cis*- and *trans*-isomers in the intermolecular interaction of the hydroxyl group with the benzene ring. The C–O bond of the horizontal *cis*-isomer is 0.0154 Å shorter than that of the monomer, while that of the horizontal *trans*-isomer is shortened only by 0.0038 Å. In addition, the degree of the variation of the C–O–H angle by the complex formation is large in the horizontal *cis*-isomer. This is probably due to the repulsion between the hydroxyl group and the benzene ring. The hydroxyl hydrogen and the hydrogen atoms of benzene cation repel each other and the repulsion may shorten the C–O single bond and enlarge the C–O–H angle. In the hori-

TABLE V. Calculated geometrical parameters of cluster species and acetic acid monomers at the CASSCF(7,7)/6-31G(d,p) level.

	Horizontal cluster		Vertical cluster	Acetic acid monomer	
	cis	*trans*	*trans*	*cis*	*trans*
R(C–H)[a]	1.0728	1.0728	1.0731		
R(C–H)[b]	1.0751	1.0751	1.0739		
R(C═O)	1.2043	1.1960	1.1980	1.1951	1.1902
R(C–O)	1.3231	1.3403	1.3376	1.3385	1.3441
R(O–H)	0.9472	0.9450	0.9450	0.9472	0.9429
R(C–C)[c]	1.4985	1.5031	1.5028	1.5010	1.5089
R(C–H)[d]	1.0800	1.0791	1.0789	1.0802	1.0796
R(C–H)[e]	1.0834	1.0852	1.0853	1.0840	1.0859
α(O–C═O)	122.2394	118.3665	118.6151	122.2051	119.9548
α(C–C═O)	125.3561	124.7704	124.5056	125.6422	124.2604
α(C–O–H)	110.5537	112.9698	112.5781	108.5520	112.0483
R(C–H···O═C)[f]	2.3862	2.3218	2.5457		
R(C–H···O═C)[g]	2.4508	2.5962	3.4300		
R(C···O═C)[h]	3.1164	3.1073	2.6170		
R(C–H···O–C)[i]	4.1951	2.5692	4.1248		
R(C···O–C)[j]	5.1169	3.6232	3.6158		
R(C–H···H–O)[k]	3.7452	3.4351	4.7506		

[a]The shortest bond in the benzene ring.
[b]The longest bond in the benzene ring.
[c]The C–C bond of acetic acid.
[d]The C–H bond of acetic acid in the plane of the carboxyl group.
[e]C–H bonds of acetic acid out of the plane of the carboxyl group.
[f]Intermolecular H···O distance between the carbonyl oxygen and the nearest hydrogen atom of the benzene ring.
[g]Intermolecular H···O distance between the carbonyl oxygen and the second nearest hydrogen atom of the benzene ring.
[h]Intermolecular C···O distance between the carbonyl oxygen and the nearest carbon atom of the benzene ring.
[i]Intermolecular H···O distance between the hydroxyl oxygen and the nearest hydrogen atom of the benzene ring.
[j]Intermolecular C···O distance between the hydroxyl oxygen and the nearest carbon atom of the benzene ring.
[k]Intermolecular H···H distance between the hydroxyl hydrogen and the nearest hydrogen atom of the benzene ring.

zontal *trans*-isomer, the hydroxyl hydrogen is on the opposite side to the benzene ring and the hydroxyl oxygen which is partially negatively charged is close to the hydrogen atoms of benzene cation. Therefore the repulsion mentioned above is weak in the horizontal *trans*-isomer. The intermolecular C–H···O–C bond length is 2.5692 Å in the horizontal *trans*-isomer, while that of the horizontal *cis*-isomer is 4.1951 Å. The O–C═O angle is also varied largely in the horizontal *trans*-isomer. This suggests that the hydroxyl oxygen interacts with the hydrogen atom of benzene cation and the additional hydrogen bond is formed between them in the horizontal *trans*-isomer. Thus the increment in the binding energy of the horizontal *trans*-isomer is attributed to this additional C–H···O–C hydrogen bond and the weakened hydrogen–hydrogen repulsion.

The intermolecular binding energy of the vertical complex is larger than those of the horizontal complexes where the double or triple hydrogen bonds are formed, although only one hydrogen atom of the benzene cation is located near the hydroxyl oxygen in the vertical *trans*-isomer. In the vertical *trans*-isomer, the carbonyl oxygen interacts with the benzene ring from the vertical direction at an intermolecular C···O═C distance as close as 2.6170 Å. This indicates that the carbonyl oxygen interacts strongly with the π-electron system of the benzene cation. The binding energy of the vertical *trans*-isomer cannot be explained only by electrostatic interaction like the horizontal complexes, since the overlap of nonbonding orbitals of the carbonyl group with π-orbitals of benzene cation can change the electronic structures. We shall try to give a more detailed discussion on this point in a later section.

3. Comparison between the results from CASSCF and DFT calculations

Geometry optimizations were also performed at the B3LYP/6-31G(d,p) level. Three optimized geometries are obtained in agreement with the CASSCF calculations. The total energies of these isomers of $(CH_3COOH)\cdot(C_6H_6)^+$ are listed in Table I. Those of acetic acid monomers and the benzene monomer cation are shown in Table II. At the B3LYP/6-31G(d,p) level, the most and least stable species is the vertical *trans*-isomer and the horizontal *trans*-isomer, respectively. This result agrees with that obtained at the CASSCF(7,7) level. Energy gaps between the *cis*- and *trans*-isomers at the B3LYP/6-31G(d,p) level are listed in Table III. The value for the horizontal complex is 798 cm^{-1} after ZPVE correction. This is 366 cm^{-1} larger than that obtained at the CASSCF(7,7) level. In contrast, the energy gap between the *trans*- and the *cis*-isomers of acetic acid exhibits similar values at both the levels of the methods: 2075 cm^{-1} at the B3LYP/6-31G(d,p) level and 2116 cm^{-1} at the CASSCF(7,7) level after the ZPVE correction. The binding energies of $(CH_3COOH)\cdot(C_6H_6)^+$ at the B3LYP/6-31G(d,p) level are shown in Table IV. The intermolecular interaction at the B3LYP/6-31G(d,p) level is estimated to be weaker than that at the CASSCF(7,7) level. However the relative tendency is in the consistent with the CASSCF calculations; the vertical complex has binding energy larger than those of the horizontal complexes and the *trans*-isomer can form stronger intermolecular binding than the *cis*-isomer. The optimized geometrical parameters at the B3LYP/6-31G(d,p) level are collected in Table VI. Intramolecular bond lengths except that of the C–O bond of the vertical *trans*-isomer are estimated to be longer at the B3LYP/6-31G(d,p) level relative to those obtained by the CASSCF calculations. On the other hand, the intermolecular distances become short by approximately 0.1 and 0.2 Å in the horizontal *cis*- and vertical *trans*-isomers, respectively. In contrast, the intermolecular distance between the benzene ring and the hydroxyl group of the horizontal *trans*-isomer at the B3LYP/6-31G(d,p) level is approximately 0.5 Å longer than that obtained at the CASSCF(7,7) level.

4. Comparison between calculated and observed vibrational spectra

Table VII shows the calculated frequencies and IR intensities of the C–H and O–H stretching vibrations of the three $(CH_3COOH)\cdot(C_6H_6)^+$ isomers and the two acetic acid isomers at the B3LYP/6-31G(d,p) level. The frequencies were also calculated at the CASSCF(7,7)/6-31G(d,p) level and they are higher than those obtained at the B3LYP/6-31G(d,p) level for all the vibrational modes shown here. In

TABLE VI. Calculated geometrical parameters of cluster species and acetic acid monomers at the B3LYP/6-31G(d,p) level.

	Horizontal cluster		Vertical cluster	Acetic acid monomer	
	cis	*trans*	*trans*	*cis*	*trans*
R(C–H)[a]	1.0841	1.0841	1.0828		
R(C–H)[b]	1.0864	1.0871	1.0861		
R(C═O)	1.2238	1.2155	1.2270	1.2104	1.2035
R(C–O)	1.3387	1.3493	1.3338	1.3575	1.3633
R(O–H)	0.9722	0.9693	0.9705	0.9724	0.9677
R(C–C)[c]	1.5020	1.5090	1.5066	1.5073	1.5190
R(C–H)[d]	1.0888	1.0887	1.0886	1.0891	1.0891
R(C–H)[e]	1.0938	1.0953	1.0955	1.0940	1.0957
α(O–C═O)	122.3148	118.4551	119.3970	122.4909	120.0143
α(C–C═O)	125.6639	124.6081	122.0039	126.0892	124.7190
α(C–O–H)	108.3232	111.4904	111.3016	105.8073	110.2626
R(C–H···O═C)[f]	2.2557	2.2519	2.3513		
R(C–H···O═C)[g]	2.3276	2.3208			
R(C···O═C)[h]	2.9897	2.9837	2.3754		
R(C–H···O–C)[i]	4.0674	3.0668	3.9918		
R(C···O–C)[j]	5.0099	4.1381	3.3983		
R(C–H···H–O)[k]	3.5703	4.0295	4.8404		

[a]The shortest bond in the benzene ring.
[b]The longest bond in the benzene ring.
[c]The C–C bond of acetic acid.
[d]The C–H bond of acetic acid in the plane of the carboxyl group.
[e]C–H bonds of acetic acid out of the plane of the carboxyl group.
[f]Intermolecular H···O distance between the carbonyl oxygen and the nearest hydrogen atom of the benzene ring.
[g]Intermolecular H···O distance between the carbonyl oxygen and the second nearest hydrogen atom of the benzene ring.
[h]Intermolecular C···O distance between the carbonyl oxygen and the nearest carbon atom of the benzene ring.
[i]Intermolecular H···O distance between the hydroxyl oxygen and the nearest hydrogen atom of the benzene ring.
[j]Intermolecular C···O distance between the hydroxyl oxygen and the nearest carbon atom of the benzene ring.
[k]Intermolecular H···H distance between the hydroxyl hydrogen and the nearest hydrogen atom of the benzene ring.

general, the frequencies obtained by DFT are closer to the experimental values than those calculated by the CASSCF method. Since our main concern in the observed vibrational spectrum is the assignment of the weak band located on the high frequency side of the free O–H stretching vibration, we discuss the relative values of the O–H stretching frequencies at each level of the theories. The frequencies of the O–H stretching vibration of the *trans*-isomer of acetic acid are 53 and 51 cm^{-1} higher than those of the *cis*-isomer at the CASSCF(7,7)/6-31G(d,p) and B3LYP/6-31G(d,p) levels, respectively. These values are in good agreement with the value of 59.6 cm^{-1} calculated by Turi and Dannenberg at the MP2/6-31G(d) level.[38] As mentioned in previous section, the frequency of the strongest band in the vibrational spectrum of $(CH_3COOH)\cdot(C_6H_6)^+$ is 3577 cm^{-1} that is close to the frequency of the *cis*-isomer of acetic acid. The calculated O–H stretching frequency of the horizontal *cis*-isomer is also close to that of the *cis*-isomer of acetic acid at the both levels. Therefore the strongest band at 3577 cm^{-1} is assigned to the O–H stretching vibration of the horizontal *cis*-isomer. The calculated frequencies of the O–H stretching vibrations of the horizontal and vertical *trans*-isomer are 26 and 27 cm^{-1} higher than that of the horizontal *cis*-isomer at the

TABLE VII. Calculated vibrational frequencies (cm^{-1}) and IR intensities (km/mol) of cluster species and acetic acid isomers at the B3LYP/6-31G(d,p) level.

	Horizontal cluster		Vertical cluster	Acetic acid monomer	
	cis	*trans*	*trans*	*cis*	*trans*
CH_3 sym. str.	3073	3058	3057	3067	3050
(acetic acid)	(0.505)	(0.557)	(3.335)	(1.851)	(4.319)
CH_3 asym. str.	3140	3123	3126	3133	3114
(acetic acid)	(0.143)	(1.439)	(0.006)	(5.242)	(9.431)
CH_3 sym. str.	3188	3188	3193	3185	3181
(acetic acid)	(4.808)	(0.936)	(0.528)	(5.612)	(3.927)
CH_3 sym. str.	3212	3209	3208		
(benzene cation)	(2.365)	(40.968)	(0.044)		
CH_3 asym. str.	3218	3213	3220		
(benzene cation)	(19.542)	(10.155)	(0.071)		
CH_3 sym. str.	3223	3222	3222		
(benzene cation)	(4.103)	(2.268)	(0.009)		
CH_3 asym. str.	3230	3231	3232		
(benzene cation)	(23.017)	(15.086)	(0.660)		
CH_3 sym. str.	3237	3237	3233		
(benzene cation)	(5.840)	(4.742)	(0.598)		
CH_3 sym. str.	3240	3241	3250		
(benzene cation)	(13.525)	(16.037)	(3.458)		
O–H str.	3758	3789	3780	3751	3802
(acetic acid)	(51.170)	(88.941)	(126.531)	(43.763)	(30.891)

CASSCF(7,7)/6-31G(d,p) level. At the B3LYP/6-31G(d,p) level, two *trans*-isomers also exhibit the O–H vibrational frequencies higher than the horizontal *cis*-isomer. These results suggest that the weak band at 3617 cm^{-1} can be attributed to the vertical and/or horizontal *trans*-isomers. As already mentioned, the vertical *trans*-isomer is the most stable species and the horizontal *trans*-isomer is 3053 cm^{-1} less stable than the vertical *trans*-isomer. Therefore we assign the band at 3617 cm^{-1} to the O–H stretching vibration of the vertical *trans*-isomer.

Now we have a problem on the intensities. The intensity ratio of the strongest band at 3577 cm^{-1} to that of the weak band at 3617 cm^{-1} cannot reflect the abundance of the horizontal *cis*-isomer to that of the vertical *trans*-isomer correctly. The observed IR spectrum is measured by the photodissociation spectroscopy that is related to the internal temperature of the complexes and the dissociation thresholds. The calculated binding energy of the vertical *trans*-isomer is 4737 and 2611 cm^{-1} larger than that of the horizontal *cis*-isomer at the CASSCF(7,7)/6-31G(d,p) and B3LYP/6-31G(d,p) levels, respectively. The binding energy larger than the photon energies is less preferable for the efficiency of photodissociation of the vertical *trans*-isomer. Only the species in highly vibrationally excited states can contribute to the photodissociation spectrum in this case.

B. Electronic states of $(CH_3COOH)\cdot(C_6H_6)^+$ isomers

1. Electronic spectra

The electronic spectrum of $(CH_3COOH)\cdot(C_6H_6)^+$ obtained by the photodissociation spectroscopy is shown in Fig. 6. Two distinct maxima are seen in the spectrum. One has its intensity maximum around 24 500 cm^{-1}. The other band begins at 12 000 cm^{-1} and extends to the 24 500 cm^{-1}

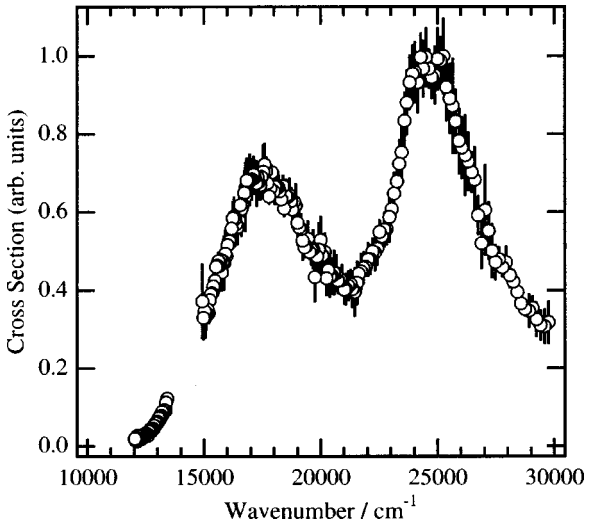

FIG. 6. Electronic spectrum of $(CH_3COOH)\cdot(C_6H_6)^+$ in the regions of 12 000–13 400 cm^{-1} and 15 000–29 600 cm^{-1} obtained by photodissociation spectroscopy.

band, with an intensity maximum around 17 500 cm^{-1}. The bandwidth of the 17 500 cm^{-1} band is approximately 5000 cm^{-1} and that of the 24 500 cm^{-1} band is 4000 cm^{-1}. The excitation energy of the 24 500 cm^{-1} band is close to that of an local excitation (LE) band of a benzene monomer cation observed in the photodissociation spectra of a series of charge resonance and charge transfer complexes with a benzene cation.[7,8,10–12] However, this assignment is dangerous for the vertical complex because the $\pi-\pi$ excited states of the vertical complex can be different from that of the benzene monomer cation due to the interaction between π-electrons of the benzene cation and nonbonding electrons of acetic acid. The band width is approximately 2.5 times wider than those of the LE bands observed in the previous works.[7,8,10–12,39] A LE band of the benzene cation in the horizontal complexes can be embedded under the 24 500 cm^{-1} band. The other band at 17 500 cm^{-1} cannot be assigned to a LE band of a component molecule, since neither this benzene cation nor acetic acid exhibits any LE band in this region. This suggests the presence of the cluster species where the electronic states are much different from those of the component molecules. The change in the electronic states can be due to the intermolecular charge transfer interaction in the cation complex. The spectral feature with a broad band width remind us a similar broadness of the CR band of a benzene dimer cation.[10–12] The nature of the charge transfer interaction is highly related to the geometry of the cation complex.

2. Calculated electronic states

The presence of the two isomers (the horizontal *cis*-isomer and the vertical *trans*-isomer) of $(CH_3COOH)\cdot(C_6H_6)^+$ is revealed by the vibrational spectrum and *ab initio* molecular orbital calculations discussed in the previous section. We investigate the electronic states of the two isomers using the multiconfiguration self-consistent field (MCSCF) calculations with the active space which consists of eleven electrons and ten orbitals. The results from the calculations with MCQDPT are applied for elucidating the experimental observation. Nakano *et al.* demonstrated that the first $\pi-\pi$ transition of cyclopentadiene is calculated to be 5.27 eV at the MCQDPT level,[40] while the two groups reported the experimental values to be 5.26 (Ref. 41) and 5.34 eV.[42]

The six valence π orbitals in the benzene cation are designated in the order of energy by π_1, π_2, π_3, π_4^*, π_5^*, and π_6^*, respectively. The first two are doubly occupied and the π_3 is the singly occupied molecular orbital (SOMO) in the ground state of the benzene cation. Table VIII shows the CASSCF configurations for the ground and four excited states of the horizontal *cis*-isomer. Those of the vertical *trans*-isomer are listed in Table IX. In those tables, molecular orbitals are designated by two characters such as $A\pi$. The first character (A or B) indicates the component molecule (acetic acid or benzene, respectively) and the second character designate the type of the molecular orbital (σ orbital, π orbital or nonbonding orbital); An means the non-bonding orbital of acetic acid. $(An+B\pi_1)$ and $(An-B\pi_1)$ denote the intermolecular bonding and antibonding orbitals originated from one nonbonding orbital of acetic acid and the π_1 orbital of the benzene cation, respectively. Figure 7 shows these orbitals with the π_3 orbital of the vertical *trans*-isomer. $(A\pi+B\pi_1)$ and $(A\pi-B\pi_1)$ also means intermolecular bonding and anti-bonding orbitals derived from π orbitals of the respective component molecules. The charge distributions between acetic acid and benzene in the respective states are obtained based on the Mulliken charges listed in Table X. The calculated excitation energies from the ground state to the respective excited states and the oscillator strengths of the two isomers of $(CH_3COOH)\cdot(C_6H_6)^+$ are listed in Table XI.

TABLE VIII. Main configurations of the horizontal *cis*-isomer at the CASSCF(11,10)/6-31G(d,p) level.

State	Coefficients	$B\sigma$	$A\pi+B\pi_1$	$A\pi-B\pi_1$	An	$B\pi_2$	$B\pi_3$	$B\pi_4^*$	$B\pi_5^*$	$A\pi^*$	$B\pi_6^*$
$1\,^2A''$	0.933	2	2	2	2	2	1	0	0	0	0
$2\,^2A''$	0.924	2	2	2	2	1	2	0	0	0	0
$1\,^2A'$	0.912	2	2	2	1	2	2	0	0	0	0
$3\,^2A''$	0.725	2	1	2	2	2	2	0	0	0	0
	−0.330	2	2	2	2	1	1	1	0	0	0
	0.312	2	2	1	2	2	2	0	0	0	0
	0.267	2	2	2	2	2	0	0	1	0	0
	−0.202	2	2	2	2	0	2	0	1	0	0
$2\,^2A'$	0.912	1	2	2	2	2	2	0	0	0	0

TABLE IX. Main configurations of the vertical *trans*-isomer at the CASSCF(11,10)/6-31G(d,p) level.

State	Coefficients	$B\sigma$	$A\pi$	$An+B\pi_1$	$An-B\pi_1$	$B\pi_2$	$B\pi_3$	$B\pi_4^*$	$B\pi_5^*$	$A\pi^*$	$B\pi_6^*$
$1\,^2A'$	0.931	2	2	2	2	2	1	0	0	0	0
$1\,^2A''$	0.916	2	2	2	2	1	2	0	0	0	0
$2\,^2A'$	0.784	2	2	2	1	2	2	0	0	0	0
	0.273	2	2	1	2	2	2	0	0	0	0
	0.257	2	2	2	2	1	1	0	1	0	0
	0.253	2	2	2	2	2	0	1	0	0	0
$2\,^2A''$	0.911	1	2	2	2	2	2	0	0	0	0
$3\,^2A'$	0.759	2	2	1	2	2	2	0	0	0	0
	−0.404	2	2	2	1	2	2	0	0	0	0
	0.227	2	2	2	2	2	0	1	0	0	0

The ground state of the horizontal *cis*-isomer is $1\,^2A''$ and well described by the Hartree–Fock configuration where the $B\pi_3$ orbital is SOMO. Thus 97.8% of the positive charge is localized in the benzene ring. On the other hand in the ground state of the vertical *trans*-isomer, 4.7% of the positive charge is transferred to acetic acid.

The first excited state is $2\,^2A''$ and well represented by a single $\pi-\pi$ excitation of $B\pi_2 \rightarrow B\pi_3$. The charge distribution between the component molecules is similar to that of the ground state. The transition energy from the ground state to the $2\,^2A''$ state is estimated to be 4604 cm^{-1} at the CASSCF level and 3877 cm^{-1} at the MCQDPT level. The oscillator strength is computed to be 1.5×10^{-5}. Thus this transition is forbidden.

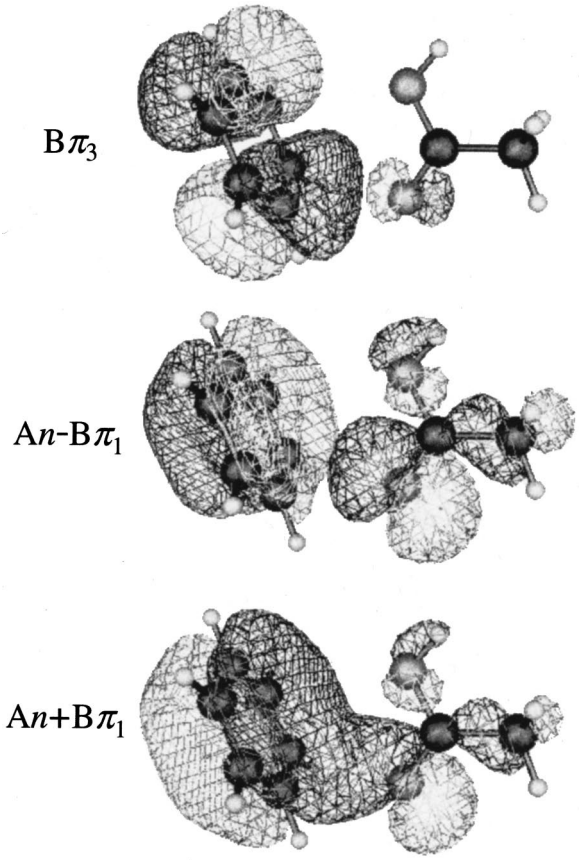

FIG. 7. Optimized molecular orbitals responsible for the charge transfer transitions of the vertical *trans*-isomer obtained by the CASSCF calculation. $(An+B\pi_1)$ and $(An-B\pi_1)$ denote the intermolecular bonding and antibonding orbitals originated from one nonbonding orbital of acetic acid and the π_1 orbital of the benzene cation, respectively.

The $1\,^2A'$ state is well represented by a single configuration where the nonbonding orbital of acetic acid is SOMO. As expected from the configuration, the positive charge is almost localized on acetic acid in the $1\,^2A'$ state. The $1\,^2A'$ state is predicted to locate at 29 172 cm^{-1} at the CASSCF level and 19 211 cm^{-1} at the MCQDPT level. The calculated oscillator strength is 0 thus the transition is completely forbidden.

The $3\,^2A''$ state comes mainly from a single $\pi-\pi$ excitation configuration of $(A\pi+B\pi_1)\rightarrow B\pi_3$. However, the state also contains a single $\pi-\pi$ excitation of $(A\pi-B\pi_1)\rightarrow B\pi_3$, two single $\pi-\pi^*$ excitation of $B\pi_2\rightarrow B\pi_4^*$ and its conjugate $B\pi_3\rightarrow B\pi_5^*$, and a double excitation of $B\pi_2\rightarrow B\pi_3$ and $B\pi_2\rightarrow B\pi_5^*$. The coefficients of the $B\pi_2\rightarrow B\pi_4^*$ and the $B\pi_3\rightarrow B\pi_5^*$ excitation have different signs from each other. According to Mulliken charges, 95.0% of the positive charge is located on the benzene ring. Therefore the $3\,^2A''$ state is the local excited state whose main character is $\pi-\pi$ excitation configuration of the benzene cation. The excitation energy to the $3\,^2A''$ state is computed to be 24 848 and 24 221 cm^{-1} at the CASSCF and MCQDPT levels, respectively. The calculated oscillator strength of 2.7×10^{-2} shows this $\pi-\pi$ transition is allowed. The result agrees with the fact that the $\pi-\pi$ transitions are observed in the spectra of cation complexes with the benzene cation.

The $2\,^2A'$ state is well described by the single $\sigma-\pi$ ex-

TABLE X. Charge distributions based on Mulliken charges.

State	Acetic acid	Benzene
	Horizontal *cis*-isomer	
$1\,^2A''$	+0.022	+0.978
$2\,^2A''$	+0.022	+0.978
$1\,^2A'$	+0.990	+0.010
$3\,^2A''$	+0.050	+0.950
$2\,^2A'$	+0.028	+0.972
	Vertical *trans*-isomer	
$1\,^2A'$	+0.047	+0.953
$1\,^2A''$	+0.019	+0.981
$2\,^2A'$	+0.300	+0.700
$2\,^2A''$	+0.023	+0.977
$3\,^2A'$	+0.697	+0.303

TABLE XI. Calculated excitation energies (cm^{-1}) and oscillator strength of $(CH_3COOH)\cdot(C_6H_6)^+$.

State		Excitation energy MCQDPT	CASSCF	Oscillator strength
		Horizontal *cis*-isomer		
$2\,^2A''$	$(\pi-\pi)$	3877	4604	1.5×10^{-5}
$1\,^2A'$	CT	19 211	29 172	0
$3\,^2A''$	$(\pi-\pi)$	24 221	24 848	2.7×10^{-2}
$2\,^2A'$	$(\sigma-\pi)$	29 542	34 168	7.5×10^{-5}
		Vertical *trans*-isomer		
$1\,^2A''$	$(\pi-\pi)$	5322	5597	7.1×10^{-5}
$2\,^2A'$	CT	11 050	23 413	5.5×10^{-2}
$2\,^2A''$	$(\sigma-\pi)$	21 397	36 751	2×10^{-6}
$3\,^2A'$	CT	28 061	29 905	6.1×10^{-2}

citation configuration of $B\sigma\rightarrow B\pi_3$. The charge distribution shows the $2\,^2A'$ state is a locally excited state. The excitation energy is computed to be 34 168 cm^{-1} at the CASSCF level and 29 542 cm^{-1} at the MCQDPT level. The calculated oscillator strength of 7.5×10^{-5} suggest the $\sigma-\pi$ transition to the $2\,^2A'$ state is forbidden.

The ground state of the vertical *trans*-isomer is well represented by the Hartree–Fock configuration where SOMO is the $B\pi_3$ orbital. Mulliken charges show that 95.3% of the positive charge is on the benzene ring in the ground state.

The first excited state is $1\,^2A''$ and well described by a single $\pi-\pi$ excitation of $B\pi_2\rightarrow B\pi_3$. Thus this state corresponds to the $2\,^2A''$ state of the horizontal *cis*-isomer. The charge distribution shows the $1\,^2A''$ is a local excited state. The transition energy is computed to be 5597 cm^{-1} and 5322 cm^{-1} at the CASSCF and MCQDPT levels, respectively. The oscillator strength is calculated to be 7.1×10^{-5}. Thus the transition to the $1\,^2A''$ state is forbidden.

The $2\,^2A'$ state comes mainly from the two single excitation of $(An-B\pi_1)\rightarrow B\pi_3$ with a coefficient of 0.784 and $(An+B\pi_1)\rightarrow B\pi_3$ with a weight of 0.273. The two single $\pi-\pi^*$ excitations of $B\pi_3\rightarrow B\pi_4^*$ and $B\pi_2\rightarrow B\pi_5^*$ also give rise to the $2\,^2A'$ state. The charge distribution shows that 30.0% of the positive charge is on acetic acid. Thus the excitation from the ground state to the $2\,^2A'$ state accompanies the charge transfer from the benzene cation to acetic acid. The transition energy is estimated to be 11 050 cm^{-1} at the MCQDPT level, while that obtained by the CASSCF method is 29 172 cm^{-1}. The discrepancy in the transition energy shows that the recovery of dynamical correlation energy in MCSCF wave function is important for this state. The calculated oscillator strength is 5.5×10^{-2}. This indicates that the charge transfer transition to the $2\,^2A'$ state can be observed.

The $2\,^2A''$ state is well represented by the single $\sigma-\pi$ excitation of $B\sigma\rightarrow B\pi_3$. As expected, the Mulliken charge shows that the $2\,^2A''$ state is a locally excited state. The calculated excitation energy is 36 751 cm^{-1} at the CASSCF level and 29 542 cm^{-1} at the MCQDPT level, respectively. The results suggest the recovery of the dynamical correlation energy is also important for this state. The oscillator strength is estimated to be 2×10^{-6}. This $\sigma-\pi$ transition is forbidden.

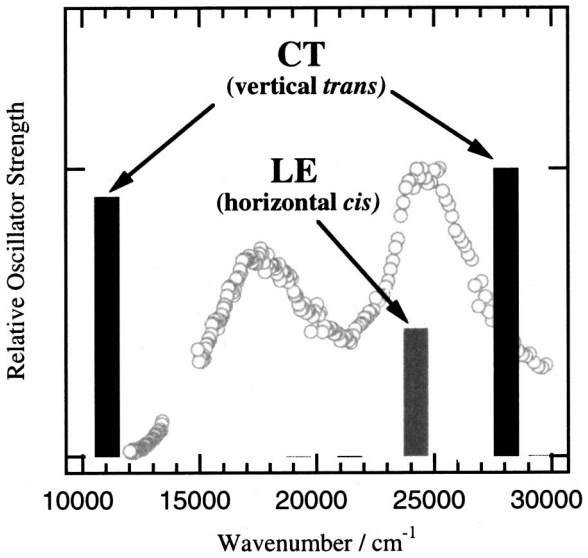

FIG. 8. Comparison between the calculated and the observed electronic spectra of $(CH_3COOH)\cdot(C_6H_6)^+$. In the calculated spectrum, population of the horizontal *cis*-isomer is supposed to be equal to that of the vertical *trans*-isomer.

The main configurations that give rise to the $3\,^2A'$ state are the same to those of the $2\,^2A'$ state. The principle configuration in the $3\,^2A'$ state is the single excitation of $(An+B\pi_1)\rightarrow B\pi_3$ with a coefficient of 0.759. The single excitation of $(An-B\pi_1)\rightarrow B\pi_3$ with a weight of -0.404 is the second most efficient configuration. The charge distribution shows the $3\,^2A'$ state also has the charge transfer character. The transition energy is computed to be 29 905 cm^{-1} and 28 061 cm^{-1} at the CASSCF and MCQDPT levels, respectively. The calculated oscillator strength of 6.1×10^{-2} suggests that the charge transfer transition to the $3\,^2A'$ state is allowed.

3. Comparison between calculated and observed electronic spectra

On the basis of the comparison between the observed spectrum of $(CH_3COOH)\cdot(C_6H_6)^+$ and the spectra of the charge resonance and charge transfer complexes with a benzene cation, we have assigned in the previous section that the LE bands of the benzene cation in the horizontal complex is embedded under the 24 500 cm^{-1} band. The 17 500 cm^{-1} band can be attributed to the CT band. The calculated electronic spectra of the two isomers are obtained using the calculated transition energies and oscillator strengths mentioned in previous section. Figure 8 shows the calculated spectrum where populations of the two isomers are supposed to be equal. For comparison, the observed spectrum is also displayed in Fig. 8. The computational results suggest that only three electronic transitions can be observed in this region. One is the $\pi-\pi$ transition of the horizontal *cis*-isomer and the others are the two charge transfer transitions of the vertical *trans*-isomer. The excitation energy of the $\pi-\pi$ transition of the horizontal *cis*-isomer is estimated to be 24 221 cm^{-1} at the MCQDPT level and correspond to the observed band at 24 500 cm^{-1}. By considering the analysis of the vi-

brational spectrum, we assign the 17 500 cm^{-1} band to one of the charge transfer transitions of the vertical *trans*-isomer. The other charge transfer transition is characterized by the excitation from an intermolecular bonding orbital, $(An + B\pi_1)$, to the $B\pi_3$ orbital that has intermolecular antibonding character, as already shown in Fig. 7. This transition can be accompanied with large geometrical change along the intermolecular coordinates. Therefore the CT band which arises from this transition can be broader than the band at 17 500 cm^{-1}. On the basis of the present calculation and the broadness of the band, the 24 500 cm^{-1} band can be assigned to the second CT band. However, the IR study also suggests the presence of the LE band of the horizontal *cis*-isomer in the same region.

V. CONCLUSION

The geometrical structures and the electronic states of $(CH_3COOH)\cdot(C_6H_6)^+$ were studied experimentally and theoretically. Experimentally, the vibrational spectrum of $(CH_3COOH)\cdot(C_6H_6)^+$ in the supersonic jet was measured in the 3000–3680 cm^{-1} region using the photodissociation spectroscopy. The electronic spectrum was also observed in the 12 000–13 400 and 15 000–29 600 cm^{-1} regions. Theoretically, *ab initio* molecular orbital calculations were performed for geometry optimizations, vibrational frequency calculations and electronic transition energy calculations. The vibrational spectrum shows two distinct bands in the O–H stretching vibrational region. The frequency of the strong band (3577 cm^{-1}) is close to that of acetic acid and the weak one is located at 3617 cm^{-1}. On the basis of geometry optimizations and frequency calculations, the strong band is assigned to the O–H stretching vibration of the horizontal *cis*-isomer where the *cis*-isomer and the benzene cation are on the same plane and the hydrogen bonds are formed between the hydrogen atoms of the benzene cation and the carbonyl oxygen of acetic acid. The weak one is assigned to the vertical *trans*-isomer where the two oxygen atoms of the *trans*-isomer of acetic acid interact with the π-electron system of the benzene cation. The weakness of the high frequency band in the photodissociation spectrum is attributed to the binding energy larger than the photon energy injected. Only hot vertical *trans*-isomers can be dissociated by the IR excitation. The electronic spectrum exhibits two bands with intensity maxima at 17 500 cm^{-1} and 24 500 cm^{-1}. The calculations of electronic excitation energies and oscillator strengths suggest the CT bands of the vertical *trans*-isomer can be observed in this region in addition to a LE band of the horizontal *cis*-isomer. The appearance of the band due to the vertical *trans*-isomer suggests that the interaction between the π orbitals of the benzene cation and the nonbonding orbital of acetic acid is as strong as the double hydrogen bonds in the horizontal complex.

[1] Z. S. Derewenda, L. Lee, and U. Derewenda, J. Mol. Biol. **252**, 248 (1995).
[2] K. Kosugi, T. Nakabayashi, and N. Nishi, Chem. Phys. Lett. **291**, 253 (1998).
[3] T. Nakabayashi, K. Kosugi, and N. Nishi, J. Phys. Chem. A **103**, 8595 (1999).
[4] N. Nishi, T. Nakabayashi, and K. Kosugi, J. Phys. Chem. A **103**, 10851 (1999).
[5] J. P. Gallivan and D. A. Dougherty, J. Am. Chem. Soc. **122**, 870 (2000).
[6] J. W. Caldwell and P. A. Kollman, J. Am. Chem. Soc. **117**, 4177 (1995).
[7] M. Matsumoto, Y. Inokuchi, K. Ohashi, and N. Nishi, J. Phys. Chem. A **101**, 4574 (1997).
[8] K. Ohashi, Y. Nakane, Y. Inokuchi, Y. Nakai, and N. Nishi, Chem. Phys. **239**, 429 (1998).
[9] K. Ohashi, H. Izutsu, Y. Inokuchi, K. Hino, N. Nishi, and H. Sekiya, Chem. Phys. Lett. **321**, 406 (2000).
[10] K. Ohashi and N. Nishi, J. Chem. Phys. **95**, 4002 (1991).
[11] K. Ohashi and N. Nishi, J. Phys. Chem. **96**, 2931 (1992).
[12] K. Ohashi, Y. Nakai, T. Shibata, and N. Nishi, Laser Chem. **14**, 3 (1994).
[13] K. Ohashi, Y. Inokuchi, and N. Nishi (unpublished).
[14] A. Fujii, A. Iwasaki, K. Yoshida, T. Ebata, and N. Mikami, J. Phys. Chem. A **101**, 1798 (1997).
[15] K. Ohashi, Y. Inokuchi, H. Izutsu, K. Hino, N. Yamamoto, N. Nishi, and H. Sekiya, Chem. Phys. Lett. **323**, 43 (2000).
[16] T. Nakanaga, P. K. Chowdhury, F. Ito, K. Sugawara, and H. Takeo, J. Mol. Struct. **413/414**, 205 (1997).
[17] K. Kimura, S. Katsumata, T. Yamazaki, and H. Wakabayashi, J. Electron Spectrosc. Relat. Phenom. **6**, 41 (1975).
[18] R. Neuhauser, K. Siglow, and H. J. Neusser, J. Chem. Phys. **106**, 896 (1997).
[19] P. Imhof, W. Roth, C. Janzen, D. Spangenberg, and K. Kleinermanns, Chem. Phys. **242**, 141 (1999).
[20] P. Imhof, W. Roth, C. Janzen, D. Spangenberg, and K. Kleinermanns, Chem. Phys. **242**, 153 (1999).
[21] M. J. Frisch, G. W. Trucks, H. B. Schlegel *et al.*, GAUSSIAN 98, Revision A.7 (Gaussian, Inc., Pittsburgh, Pennsylvania, 1999).
[22] Alex A. Granovsky, http://classic.chem.msu.su/gran/gamess/index.html
[23] M. W. Schmidt, K. K. Baldridge, J. A. Boatz *et al.*, J. Comput. Chem. **14**, 1347 (1993).
[24] A. D. Becke, J. Chem. Phys. **98**, 5648 (1993).
[25] C. Lee, W. Yang, and R. G. Parr, Phys. Rev. B **37**, 785 (1988).
[26] B. Miehlich, A. Savin, H. Stoll, and H. Preuss, Chem. Phys. Lett. **157**, 200 (1989).
[27] H. Nakano, J. Chem. Phys. **99**, 7983 (1993).
[28] R. S. Mulliken, J. Chem. Phys. **23**, 1833 (1955).
[29] R. S. Mulliken, J. Chem. Phys. **23**, 1841 (1955).
[30] R. S. Mulliken, J. Chem. Phys. **23**, 2338 (1955).
[31] R. S. Mulliken, J. Chem. Phys. **23**, 2343 (1955).
[32] B. M. Bode and M. S. Gordon, J. Mol. Graphics **16**, 133 (1998).
[33] W. Weltner, J. Am. Chem. Soc. **77**, 3941 (1955).
[34] M. Haurie and A. Novak, J. Chim. Phys.-Chim. Biol. **62**, 137 (1965).
[35] J. K. Wilmshurst, J. Chem. Phys. **25**, 1171 (1956).
[36] R. H. Page, U. R. Shen, and U. T. Lee, J. Chem. Phys. **88**, 5362 (1988).
[37] A. Fujii, E. Fujimaki, T. Ebata, and N. Mikami, J. Chem. Phys. **112**, 6275 (2000).
[38] L. Turi and J. J. Dannenberg, J. Phys. Chem. **97**, 12197 (1993).
[39] Y. Inokuchi, K. Ohashi, M. Matsumoto, and N. Nishi, J. Phys. Chem. **99**, 3416 (1995).
[40] H. Nakano, T. Tsuneda, T. Hashimoto, and K. Hirao, J. Chem. Phys. **104**, 2312 (1995).
[41] R. P. Frueholz, W. M. Flicker, O. A. Mosher, and A. Kuppermann, J. Chem. Phys. **70**, 2003 (1979).
[42] W. C. Price and A. D. Walsh, Proc. R. Soc. London, Ser. A **179**, 201 (1941).